4-2013

The vocal mechanism of two songbirds, the Bengalese Finch (Lonchura striata) and the Northern Cardinal (Cardinalis cardinalis): 3D modeling of complex skeleto-muscular systems based on computer visualization and animation of x-ray CT data

Caroline Blevins

The vocal mechanism of two songbirds, the Bengalese Finch (*Lonchura striata)* and the Northern Cardinal (*Cardinalis cardinalis*): 3D modeling of complex skeleto-muscular systems based on computer visualization and animation of x-ray CT data

by

Caroline Elizabeth Blevins

Undergraduate honors thesis under the direction of

Dr. Dominique G. Homberger

Department of Biological Sciences

Submitted to the LSU Honors College in partial fulfillment of the Upper Division Honors Program.

April 2013

Louisiana State University
& Agricultural and Mechanical College
Baton Rouge, Louisiana

Acknowledgements

First, I would like to thank Dr. Dominique G. Homberger for being a great teacher and mentor these past few years. She has provided me with indispensable advice and support while profoundly impacting my interest in research. I also would like to thank Dr. Les Butler (Department of Chemistry, LSU, Baton Rouge), as well as Dr. Homberger, for fueling my interest in visualization during their 3D imaging class in the spring of 2011. And I would like to thank Dr. Jinghua Ge for her significant effort on and crucial contribution to the project. She has spent countless hours developing the technique for and working on the "character rigging" of the 3D model of the Cardinal.

Work with the Northern Cardinal data would not have been possible without the audio and x-ray video data of a vocalizing Northern Cardinal by Dr. Roderick A. Suthers (Department of Biology, Indiana University, Bloomington) and the synchronizing of the x-ray video with audio files by John Rothgerber in Dr. Suthers's lab. Dr. Kenneth L. Matthews II (Department of Physics & Astronomy, LSU, Baton Rouge) acquired the high-resolution x-ray CT data of the head of the Bengalese Finch. Dr. J. Michael Mathis (Gene and Cell Therapy Program, LSU Health Sciences Center, Shreveport) acquired the x-ray CT data of the Bengalese Finch and Northern Cardinal.

I am very grateful to Jonathan A. Bonin and Dr. Michelle L. Osborn for their support and assistance during the past two years. I would also like to thank all of the lab members in the Homberger lab, especially the lab manager Sigrid N. Hamilton, for their help with my research and thesis, as well as for their continued support.

Finally, I would like to thank Louisiana State University for providing me with funding through the Chancellor's Future Leaders in Research Program.

Abstract

Songbirds provide an excellent model for human vocalization. In humans, sound that is generated in the larynx is filtered and modulated by intricate movements within the supralaryngeal and oral cavities which affect the resonance properties of the vocal tract. In birds, the syrinx is analogous to the larynx: Sound that is generated in the syrinx is filtered and modulated by intricate movements within the tracheal, laryngeal and oral cavities. Since the physical mechanism by which complex sounds are generated is similar in both organisms, creating a biomechanical model of the vocal tract of a songbird will allow for a greater understanding of the production of human speech. To this effect, virtual three-dimensional models of the numerous skeletal elements of the head, neck, tongue, larynx and trachea of two songbird species, a Bengalese Finch (*Lonchura striata*) and a Northern Cardinal (*Cardinalis cardinalis*), were created from x-ray CT scans with a visualization program. The 3D model of the Cardinal was mobilized with an animation program and registered with a 2D digital x-ray video of a vocalizing bird. The animated 3D model allows an analysis of the changing spatial relationships among the various elements of the jaw, hyoid, laryngeal, tracheal and cervical apparatus during vocalization and their effects on the sound quality.

Introduction

Songbirds have been used as a model species to understand the biomechanics and neural control of human vocalization for several years (Riede 2006). In humans, the voice is produced by the vocal folds in the larynx. As a person exhales, air pressure building up beneath the glottis causes the vocal folds to open. As the upper edges of the folds finish opening, the lower edges begin to close again due to the Bernoulli Effect (Sataloff 1992). This rippling produces an acoustic vibration (Doupe & Kuhl 1999). Sound is modulated by movements within the supralaryngeal and oral cavities, which affect the resonance properties of the vocal tract. In birds, the syrinx is analogous to the larynx in mammals in terms of sound production. It is located at the bifurcation of the trachea and comprises membranes that are analogous to the vocal folds in humans (Podos 1995, Riede 2006). Sounds are modulated by movements of the neck, trachea, larynx, tongue, and beak (Doupe & Kuhl 1999; Homberger 1999). The complex structure of the larynx corresponds to that of the supralaryngeal cavities in humans and enables parrots and some songbirds to mimic human speech (Homberger 1999). Until recently, the study of the mechanism of vocalization has been hampered by the inaccessibility of the vocal tract within the respiratory tract of live birds. The invention of x-ray CT scanning allowed research on vocalization in birds and mammals to reach a new level of understanding.

X-rays were discovered by the physicist Wilhelm Roentgen in 1895 during experiments with a cathode ray generator, which showed that the rays easily pass through certain materials, such as soft tissues, but are absorbed by other materials, such as bone and metals (Bradley 2008). Shortly afterwards, Roentgen released an x-ray image of his wife's hand, demonstrating that this new form of electromagnetic radiation had promising applications for the medical field (Assmus 1995). Almost immediately, x-rays became widely used as a noninvasive method of diagnosis.

However, there were limitations to this new technology as early x-ray images required development in a dark room and lacked detail (Bradley 2008). The introduction of computers in the second half of the twentieth century paved the way for an improvement in x-ray imaging technology.

X-ray CT (computed tomography) scanning was first developed in 1972 by Godfrey Hounsfield as a way of visualizing the interior of an object by taking x-ray images from various angles (Bradley 2008). Although the first CT scanner that was designed by Hounsfield was able to scan objects only up to of the size of a human head, a full-body CT scanner was developed several years later (Beckmann 2009). Since then, major advances have been made in x-ray CT technology. For example, the time needed to acquire a sufficient number of slices to complete a 3D reconstruction of the data has decreased from hours to seconds (Bradley 2008). This time saving, combined with a considerable increase in image resolution and computing power, has made x-ray CT scanning an invaluable tool for both medicine and research.

All x-ray imaging is based on the differential absorption of x-rays by an object. The x-ray source emits radiation of known strength, and the object absorbs some of it. In a standard, non-digital x-ray machine, a plate situated behind the object captures the x-rays that have passed through the object (Bradley 2008). With a CT scanner, the x-ray source rotates around the object and sends a fanned beam of x-rays through the object, while a detector records the residual x-rays (Beckmann 2009). A computer integrates the data and produces a series of cross-sectional slices (x-ray images) of the object. The quality of the data acquired from a CT scanner depends on the intensity of the x-rays emitted as well as on the size of the imaging chamber and the number of slices produced.

Once the CT data have been acquired, they can be imported into a computer program, such as Avizo®[1], which visualizes the cross-sectional slices of the object and allows the reconstruction of the CT data set into a 3D model of the object. In addition, Avizo allows particular parts of the CT data set to be segmented, or digitally marked and isolated, into so-called materials that can be moved into various positions independently from one another.

In order to recreate natural movements of the live animal in the 3D model of the CT scanned animal, the segmented 3D model needs to be processed by a 3D computer graphics program, such as Maya®[2], which is designed for 3D animation, rendering, and the production of visual effects. The computer animation technique called "character rigging" allows the introduction of kinematic constraints to prevent unnatural or undesirable movements (Autodesk 2012). Once the 3D model has undergone character rigging, animation of the 3D model can proceed with the help of movement controls that move the materials only at specified joints and in particular directions.

Materials and Methods

CT Data Acquisition

The bird specimens [two Bengalese Finches, *Lonchura striata* (DGH catalog # 215 and #248), and a Northern Cardinal, *Cardinalis cardinalis* (DGH catalog # 246)] that were used for acquiring the x-ray CT data sets were provided by Dr. Roderick A. Suthers (Dept. of Biological Sciences, Indiana University, Bloomington) and are housed in the collections of Dr. Dominique

[1] Visualization Sciences Group, Inc., Burlington, MA
[2] Autodesk, Inc., San Rafael, CA

G. Homberger. The x-ray CT data were acquired using two CT scanners. The high-resolution CT data from the very small head of the Bengalese Finch (DGH catalog # 215) head were acquired using the SkyScan[3] micro-CT scanner by Dr. Kenneth L. Matthews II at the Dept. of Physics & Astronomy at Louisiana State University, Baton Rouge. This system has a 40 kvP polychromatic x-ray beam, 28 mm field of view, and a 37 µm voxel length. The CT data from the whole body of the Bengalese Finch (DGH catalog # 248) and the head, neck, and shoulders of the Northern Cardinal (DGH catalog # 246) were acquired using a combined CT-PET-SPECT scanner[4] at the Louisiana State University Health Sciences Center in Shreveport. This scanner has a greater field of view, but larger voxels and, thus, a lower image resolution than the SkyScan CT scanner. This system has a beam varying from 40 to 80 kvP, 2 by 2 binning, a 1024 by 1024 projection matrix size, and a 1 mm voxel length.

An x-ray digital video of a vocalizing Northern Cardinal was provided by Dr. Roderick A. Suthers. The video (Car_542_11C) lasts for 2.6 seconds and comprises 88 individual frames at 29 frames per second, of which frames 20 through 40 were used for this study. The frame size of the video is 980 x 980 pixels. John Rothgerber (laboratory of R. A. Suthers) synchronized this video with the sonogram of the simultaneously recorded audiotape.

3D Reconstruction of the X-ray CT Data through the Software Program Avizo

Images from a CT scan are shown in grayscale with the shade of each pixel based on its intensity (usually expressed in Hounsfield units), which is dependent on how much of the x-ray

[3] Micro Photonics, Allentown, PA
[4] Gamma Medica-Ideas, Northridge, CA

radiation is absorbed by the scanned object (Figure 1). Pixels of a high intensity from materials that absorb much radiation, such as dense bone or metal, are white. Pixels of a low intensity from materials that do not absorb much radiation, such as air, are black. Pixels of soft tissues, such as connective tissue and muscle, are in various shades of gray. 3D renderings of the data set contain voxels, which are volumetric, or 3D, pixels.

Avizo offers a number of modules that, when connected to a CT data set, apply certain calculations or analytics to the data (Visualization Sciences Group 2012). The orthoslice module, for example, displays orthographic sections of a CT data set (see Figure 1). The number of slices depends on the size of the object that was CT-scanned and on the desired image resolution. Generally, a larger object will require a greater number of slices for a particular resolution.

The volume rendering module displays a 3D image based on the intensity value of each voxel. Voxels that absorb less x-rays are shown as more opaque in the image. This directly corresponds to the density of the object at that specific point. The volume rendering module is useful because the color preferences of the module can be adjusted to allow the user to view the object in varying degrees of transparency, with dense materials in the center, such as bones, visible through layers of less dense material, such as skin and soft tissue (see Figure 2).

The isosurface module allows users to view only pixels that fall within a certain range of intensities. The resulting image provides an opaque image of the surface of the scanned object (see Figure 3). The threshold value can be adjusted to produce an isosurface that is appropriate for displaying a particular tissue within an object, but it can be difficult to find the proper threshold values to clearly visually isolate a particular tissue. If the threshold is set too low,

Avizo may display unwanted objects, such as image noise, which appears as graininess or ray-like streaks in the displayed image. Image noise may be a result of a problem with the image sensor or the result of the interaction of metal objects with the x-rays during the scanning process. If the threshold is too high, some low-density parts of the tissue of interest may not be fully displayed.

The label field module allows for the segmentation of CT data sets by assigning labels to individual pixels to isolate them into particular so-called materials by marking defined regions on orthographic slices. Segmented materials, such as individual skeletal elements, may be viewed or moved independently from one another, which is a necessary condition for the process of character rigging and animation (see below). During segmentation, pixels can be selected and either added or removed from a certain material. This module has four windows (see Figure 4), one of which displays a 3D image of the object to be segmented as a reference (see Figure 4A). The other three windows show orthoslices from three perspectives: xz (horizontal sections; Figure 4B), yz (longitudinal sections; Figure 4C), and xy (transverse sections; Figure 4D). The three perspectives are useful for visualizing a particular voxel of the object in different views to ensure that it is added to the correct material during segmentation.

The surface generation module creates a triangular grid of the surface of the object using the results of an image segmentation (a label field) and the resulting image is viewed using the surface view module. This module is especially useful because it allows the user to select and visually isolate particular segmented materials. Additionally, the rendered surface can be simplified by smoothing, a process in which some triangles are removed from the image reconstruction. (see Figure 5A, B).

Avizo offers several ways to segment data. One way is through automatic segmentation by thresholding. Pixels with similar intensity values are automatically grouped together and labeled as separate materials. This process is similar to the function of the volume rendering module. One difficulty with this automatic segmentation is that it requires data with clearly defined borders between the materials that are to be segmented. CT scans of biological objects usually lack clear edges between materials due to the gradually varying densities of certain tissues. Even tissues of high density, such as bone, often have regions that are less dense and, therefore, are likely to be missed during automatic segmentation. Another difficulty is that automatic segmentation separates the data simply by x-ray absorption and emission values and combines areas of similar intensities, even if these are from different materials.

Another way to segment CT data is to use the brush tool for manual, or interactive, segmentation by highlighting certain pixels to assign them to a material. A benefit of this tool is that it allows for complete control over which pixels are selected. One drawback, however, is that selecting individual pixels is an extremely time-consuming process. A faster option is provided by the magic wand, or region growing, tool, which allows the user to specify a range of intensity values bordered by an upper and lower threshold value (see Figure 6). The tool automatically selects all pixels that fall within this range, and these pixels can then be assigned to a material. For example, the magic wand tool can be used to select all pixels that correspond to the approximate density of bone. Although the magic wand tool allows the segmentation of large regions to be completed more quickly, its exclusive use can lead to inaccurate results, because the density of a particular material may not be uniform. Many different materials were needed to create an accurate model of the head and neck that could be moved realistically. For example, each tracheal ring and each vertebra had to be labeled as individual materials.

Therefore, using a combination of the brush tool and magic wand tool can produce accurate results while expediting the segmentation process (see Figures 7-9).

Animation of a 3D Model through the Software Program Maya

Animation is the simulation of movement using rapidly displayed images and can be applied to a 3D model from x-ray CT data to simulate natural movements that could have been executed by the scanned object when alive. In order to recreate these natural movements of the various elements of an object, the 3D model needs to be processed through a 3D computer graphics program, such as Maya.

In the surface view module of Avizo, the segmented materials, such as skeletal elements, can be selected individually and saved as separate files (i.e., ".obj" files). These files can be imported into Maya, which recognizes them as individual objects and allows them to be moved separately. The computer animation technique called "character rigging" allows the introduction of kinematic constraints to reduce the freedom of movement between the various segmented materials and to prevent unnatural or undesirable movements. The technique of character rigging includes the linking of particular skeletal elements to one another, so that the movement of one element can automatically move other elements. The character rigging technique allows the various materials (i.e., skeletal elements) of the 3D model to be moved and rotated at the joints using movement control tools in Maya (see Figure 10). The character rigging of the 3D model was executed by Dr. Jinghua Ge, Advanced Visualization Service, Center for Computation and Technology, Louisiana State University, Baton Rouge.

In order to animate a segmented 3D model, reference images are needed to ensure accurate and natural movements. In this study, the x-ray video of a singing Northern Cardinal was broken down into individual images (i.e., PNG stills) that were placed in the background of each frame in Maya (see Figure 11). The 3D model was lined up with the x-ray images one frame at a time by moving the joints and skeletal elements into positions that matched those in the x-ray images. The entire scene, containing the x-ray video frames and the 3D model in various positions, can be rotated and viewed from different perspectives in space. Screenshots were taken of the 3D model from a lateral and frontal perspective, and the resulting images were imported into Windows Movie Maker to create a video that displays the movements of the 3D model. An amplitude waveform and sonogram of an audio file of the song that had been recorded simultaneously with the x-ray videotape of a Northern Cardinal, *Cardinalis cardinalis* (DGH catalog # 269) was synchronized with the video (see Figures 12-14).

Results and Discussion

3D models were created of the skeletal elements of the head, neck, tongue, larynx, trachea and shoulders of two songbirds, a Bengalese Finch, *Lonchura striata*, and a Northern Cardinal, *Cardinalis cardinalis.* The 3D models can be virtually rotated to visualize the relationships among the skeletal elements from different perspectives. Additionally, particular skeletal elements can be visually isolated by visually removing other elements, so that, for example, internal elements can be viewed.

A mobilized 3D model was created of the Northern Cardinal. After character rigging, this model was animated by registration with an x-ray video of a vocalizing bird. This allows for an

analysis of the movements of the shoulders, neck, jaw, trachea, and hyoid apparatus during sound production.

The value of this approach is that a single, lateral x-ray video can be used for the registration. This is helpful for minimizing the x-ray exposure of the subject. Additionally, it does not require the implantation of markers, which are both difficult to perform and destructive to the subject. The size of markers makes them impractical for small subjects, such as the Bengalese Finch and Northern Cardinal. Metal markers also introduce a potential source of noise in x-ray imaging and reduce the quality of the CT data. For these reasons, our 3D model registration method is especially well suited for small, delicate or rare subjects, and potentially even for humans.

In future work, the origins and insertions of muscles will be marked on the skeletal elements of the visualized 3D model to create a complete biomechanical 3D model. This model will make it possible to track the muscle contractions and movement of bones while the bird is singing. It will make it possible to measure the degree of muscle contractions and resulting forces acting on specific skeletal elements. Hence, the complete animated 3D model will be useful for analyzing the relationship between the configuration of the skeletal elements and the muscle contractions as a bird produces specific sounds. Since the mechanism of articulated sound between humans and songbirds is comparable, the modeled vocal tract of a songbird can be used as an experimental model for a greater understanding of human speech.

References

Assmus, A. (1995) Early History of X-rays. Beam Line 25 (2): 10-24.

Avizo 7 User's Guide. (2012) Visualization Sciences Group, Inc., Burlington, MA

Beckmann, E.C. (2009) CT Scanning the Early Days. British Journal of Radiology 79 (937): 5-8.

Bock, W. (1960) The Palatine Process of the Premaxilla in the Passeres. Bulletin of the Museum of Comparative Zoology 122 (8): 553-565.

Bradley, W. (2008) History of Medical Imaging. Proceedings of the American Philosophical Society 153 (2): 349-61.

Doupe, A., & P. Kuhl. (1999) Birdsong and Human Speech: Common Themes and Mechanisms. Annual Review of Neuroscience 22: 567-631.

Homberger, D.G. (1999) The avian tongue and larynx: Multiple functions in nutrition and vocalization. Pp. 94-113 *in* Proceedings of the 22nd International Ornithological Congress. (N.J. Adams & R.H. Slotow, eds.). University of Natal, Durban, South Africa.

Lima, F.C., L.G. Vieria, A.L.Q. Santos, S.B.S. De Simone, L.Q.L. Hirano, J.M.M. Silva, & M.F. Romao. (2009) Anatomy of the Scleral Ossicles in Brazilian Birds. Brazilian Journal of Morphological Sciences 26 (3-4): 165-69.

Maya 2012 User's Guide. Autodesk, Inc., San Rafael, CA.

Podos J., J.K. Sherer, S. Peters, & S. Nowicki. (1995) Ontogeny of vocal-tract movements during song production in song sparrows. Animal Behaviour 50 (5): 1287-1296.

Riede T, R.A. Suthers, N.H. Fletcher, & W. Blevins. (2006) Songbirds tune their vocal tract to the fundamental frequency of their song. Proceedings of the National Academy of Sciences 103:5543-5548.

Sataloff, R.T. (1992) The human voice. Scientific American 267 (6): 108-115.

Suthers, R.A. & S.A. Zollinger. (2007) From brain to song: The vocal organ an vocal tract. Neuroscience of birdsong (H.P. Zeigler & P. Marleer, eds.). Cambridge University Press, Cambridge, United Kingdom.

Figures

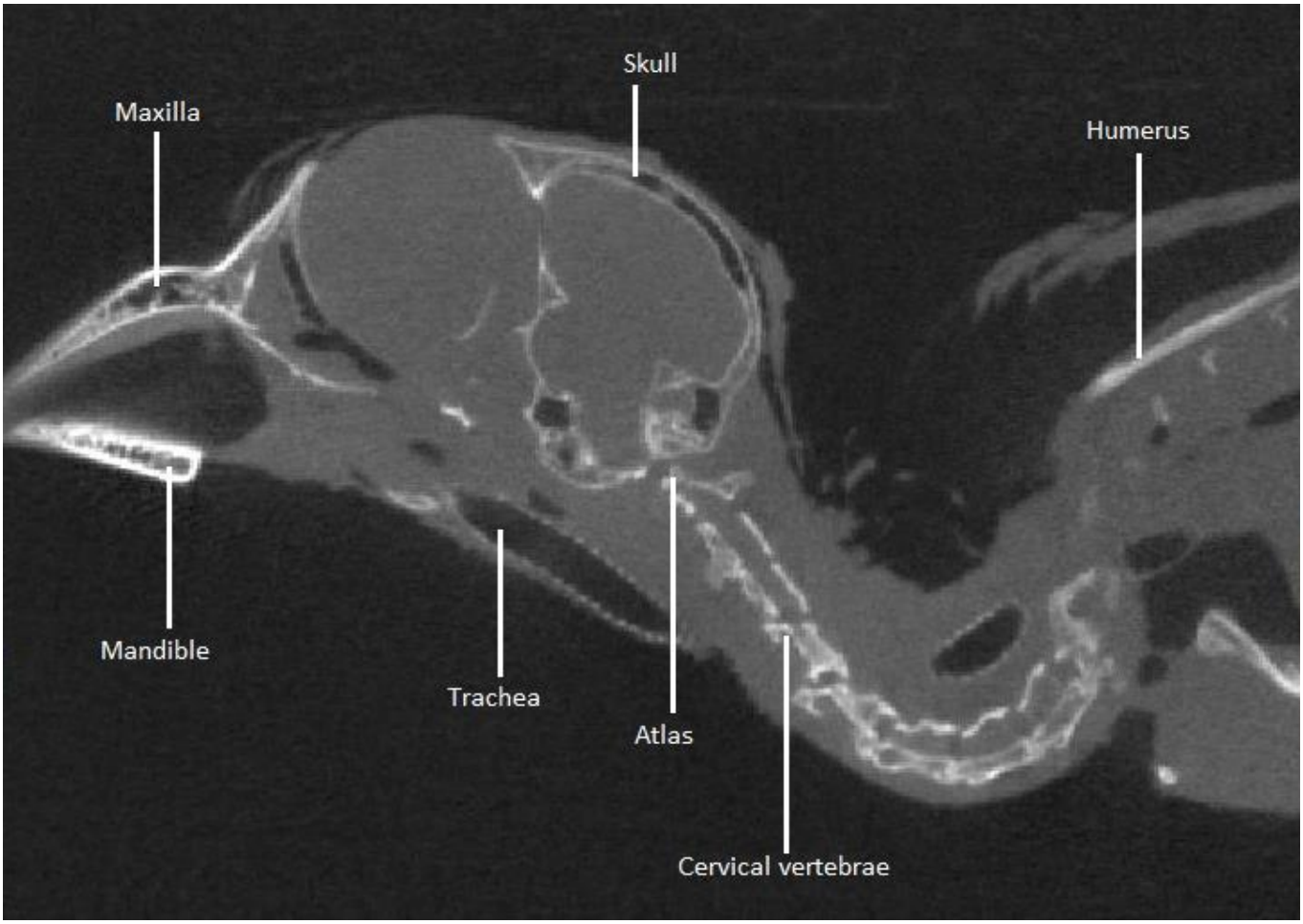

Figure 1: Screen shot of a longitudinal orthoslice in Avizo® of the head, neck and shoulder region from an x-ray CT scan of a Northern Cardinal, *Cardinalis cardinalis* (DGH catalog #246).

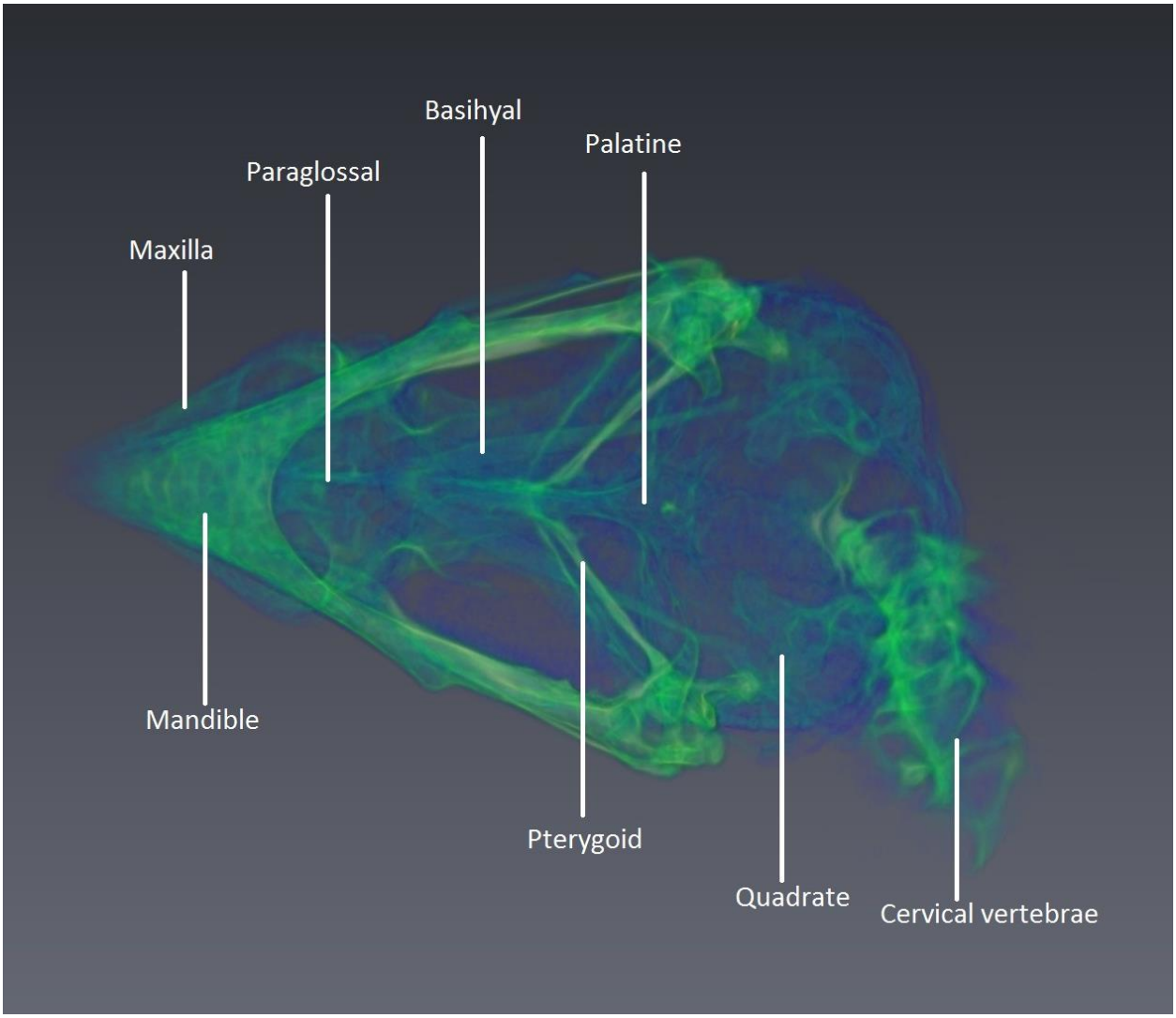

Figure 2: Screen shot of the ventral view of the volume rendering in Avizo® of the head and neck from an x-ray CT scan of a Bengalese Finch, *Lonchura striata* (DGH catalog #215). Areas of a higher density are shown in green, while areas of a lower density are shown in blue.

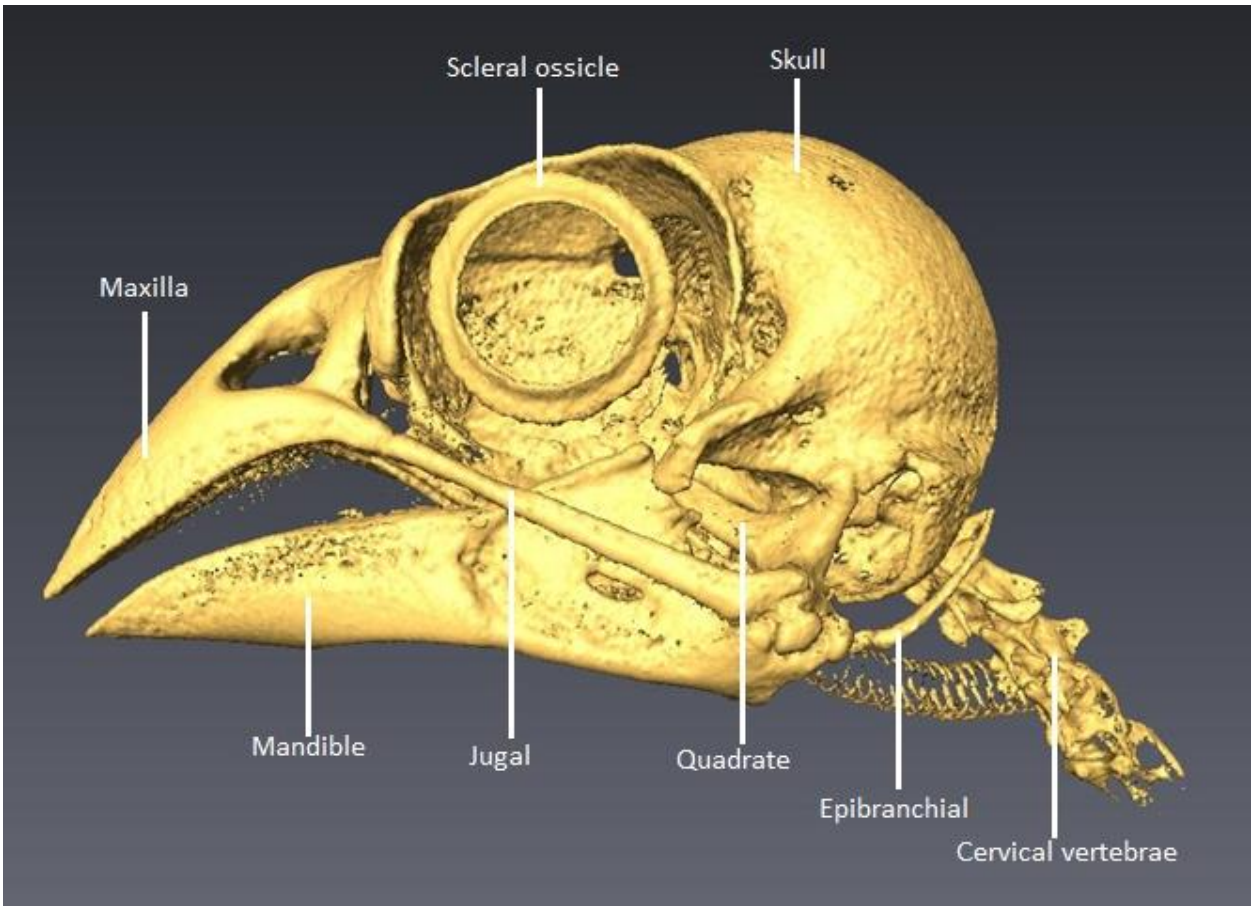

Figure 3: Screen shot of an isosurface rendering in Avizo® of the skeletal elements of the head, tongue, trachea and neck from an x-ray CT scan of the head and neck of the Northern Cardinal, *Cardinalis cardinalis* (DGH catalog #246).

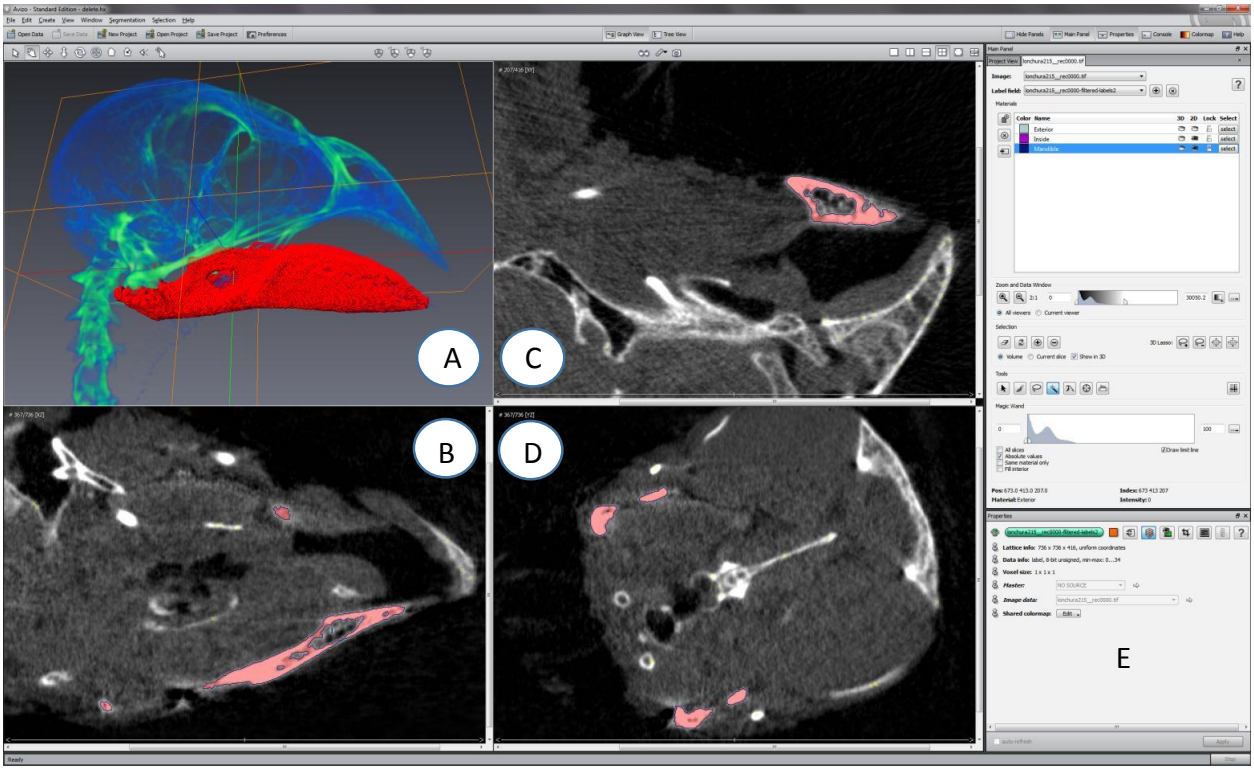

Figure 4: Screen shot of the Labelfield Module in Avizo® from an x-ray CT scan of the head and neck of the Bengalese Finch, *Lonchura striata* (DGH catalog #215); the mandible is highlighted in red (A) or pink (B-D). (A) Volume Rendering with a full segmented mandible (in red). (B) Horizontal orthoslice through the head. (C) Longitudinal orthoslice through the lower part of the head. (D) Transverse orthoslice through the skull. (E) Properties of the data set, including voxel size and image size.

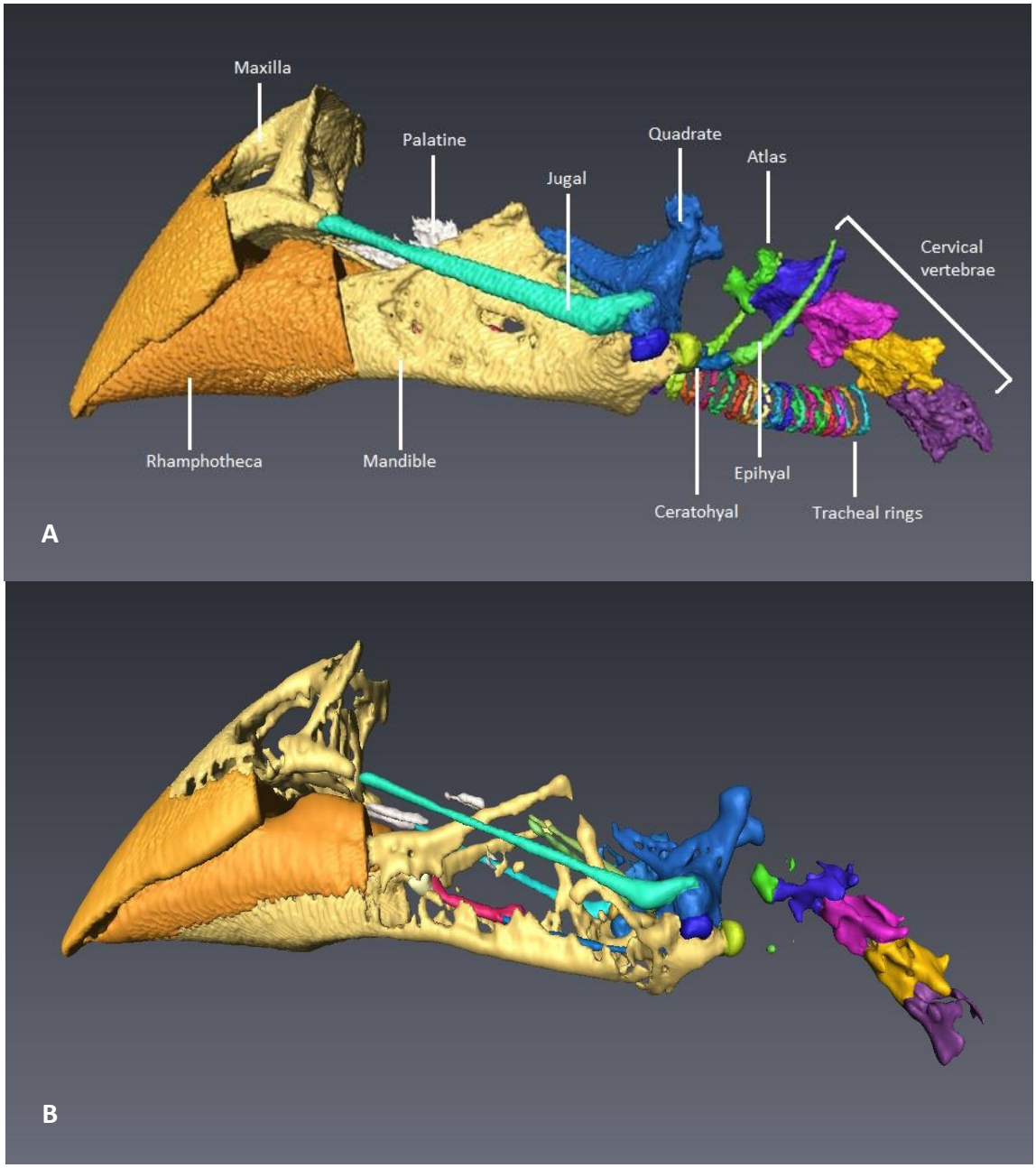

Figure 5: Screen shots of the surface generation rendering in Avizo® of the segmented skeletal elements of the jaw and hyoid apparatus, the trachea, and the five uppermost vertebrae from an x-ay CT scan of the Northern Cardinal, C*ardinalis cardinalis* (catalog # 246). (A) The surface of the skeletal elements have not undergone smoothing. (B) The surfaces of the skeletal elements have undergone unconstrained smoothing, which resulted in the loss of some pixels in the rendered image.

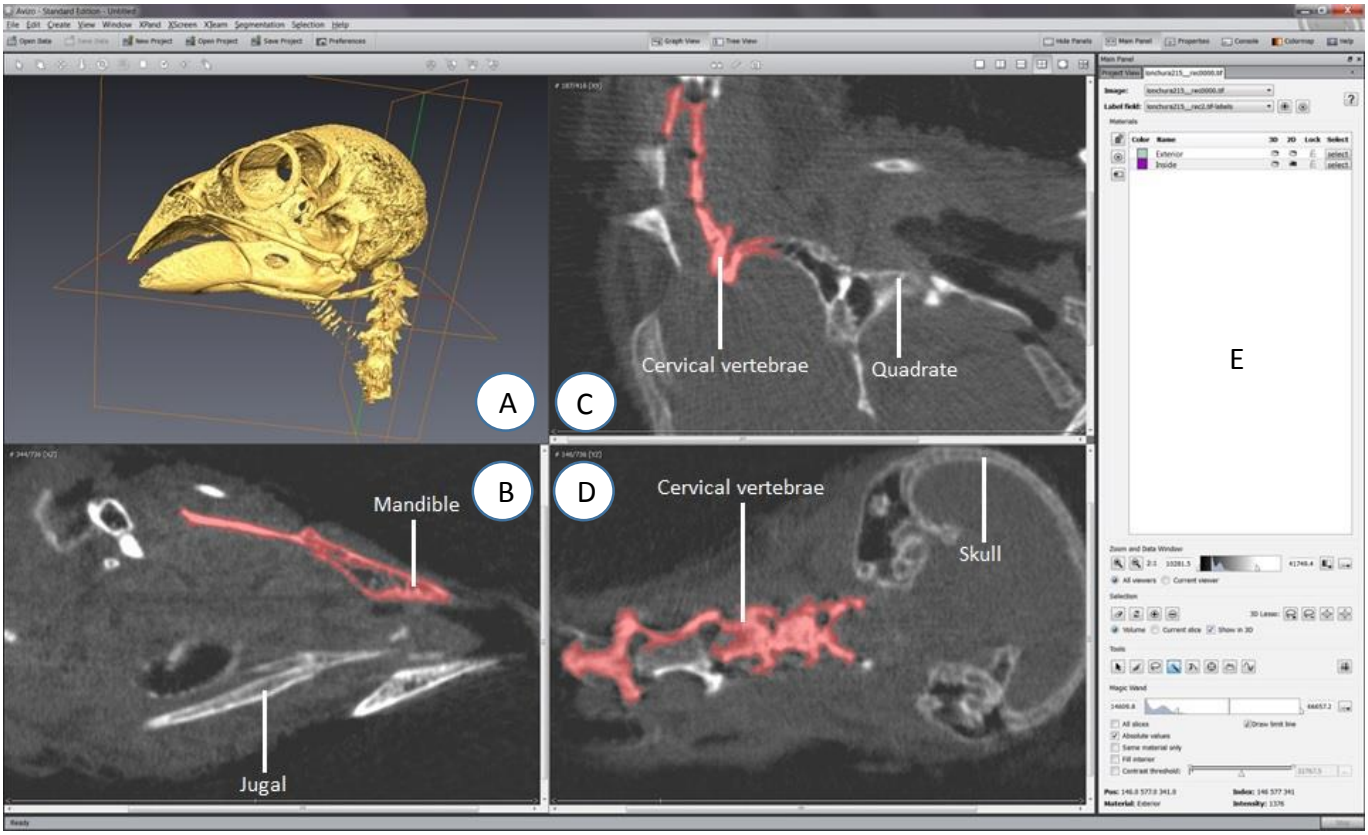

Figure 6: Screen shot of the labelfield module in Avizo® of the skeletal elements of the head, tongue, trachea and neck from an x-ray CT scan of a Bengalese Finch, *Lonchura striata* (DGH catalog #215) after application of the Magic Wand, or Region Growing Tool. (A) Isosurface rendering. (B) Horizontal orthoslice through the head. The mandible is highlighted in pink. The magic wand tool has accurately segmented the bone. (C-D) Longitudinal and transverse orthoslices through the head and neck. The vertebral column, highlighted in pink, has been segmented as a single object, despite being composed of individual bones. (E) List of materials that have been segmented. The default materials, exterior and interior, are displayed.

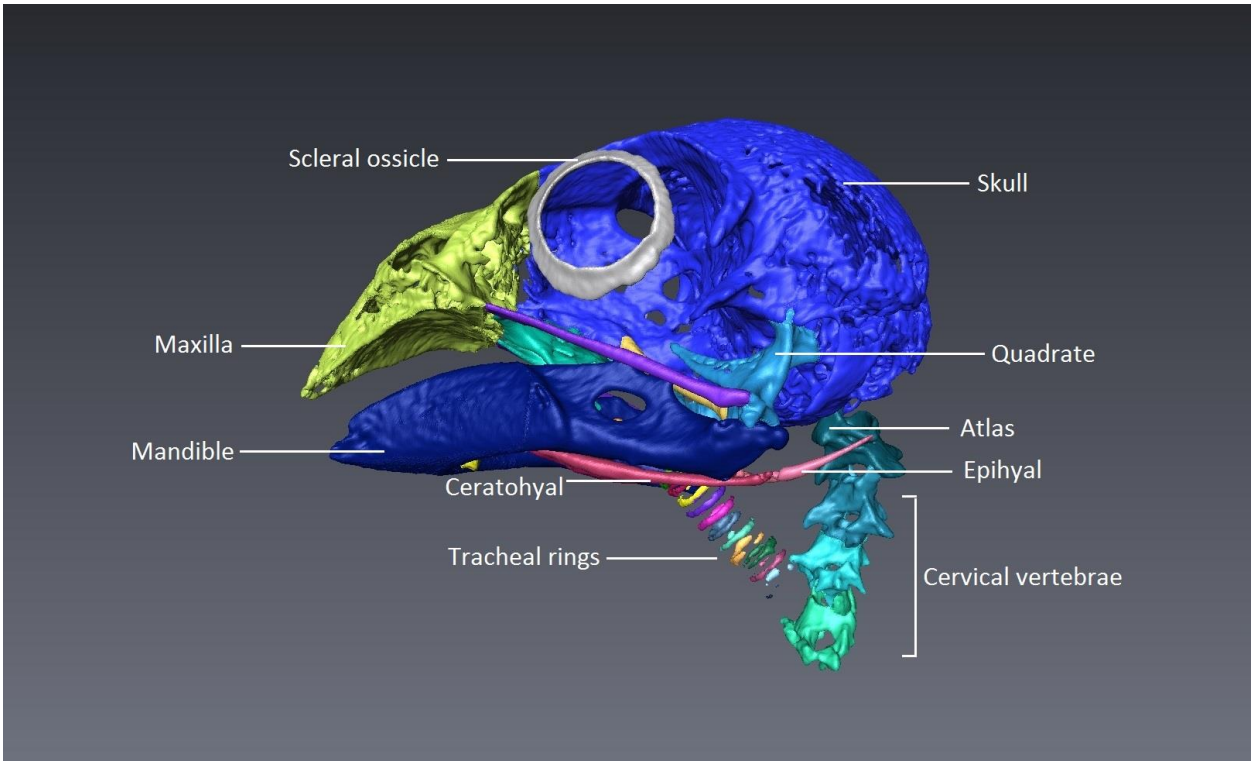

Figure 7: Screen shot of a lateral view of a surface generation rendering in Avizo® of the segmented skeletal elements of the head, neck, trachea, and hyoid from an x-ray CT scan of a Bengalese Finch, *Lonchura striata* (DGH catalog #215).

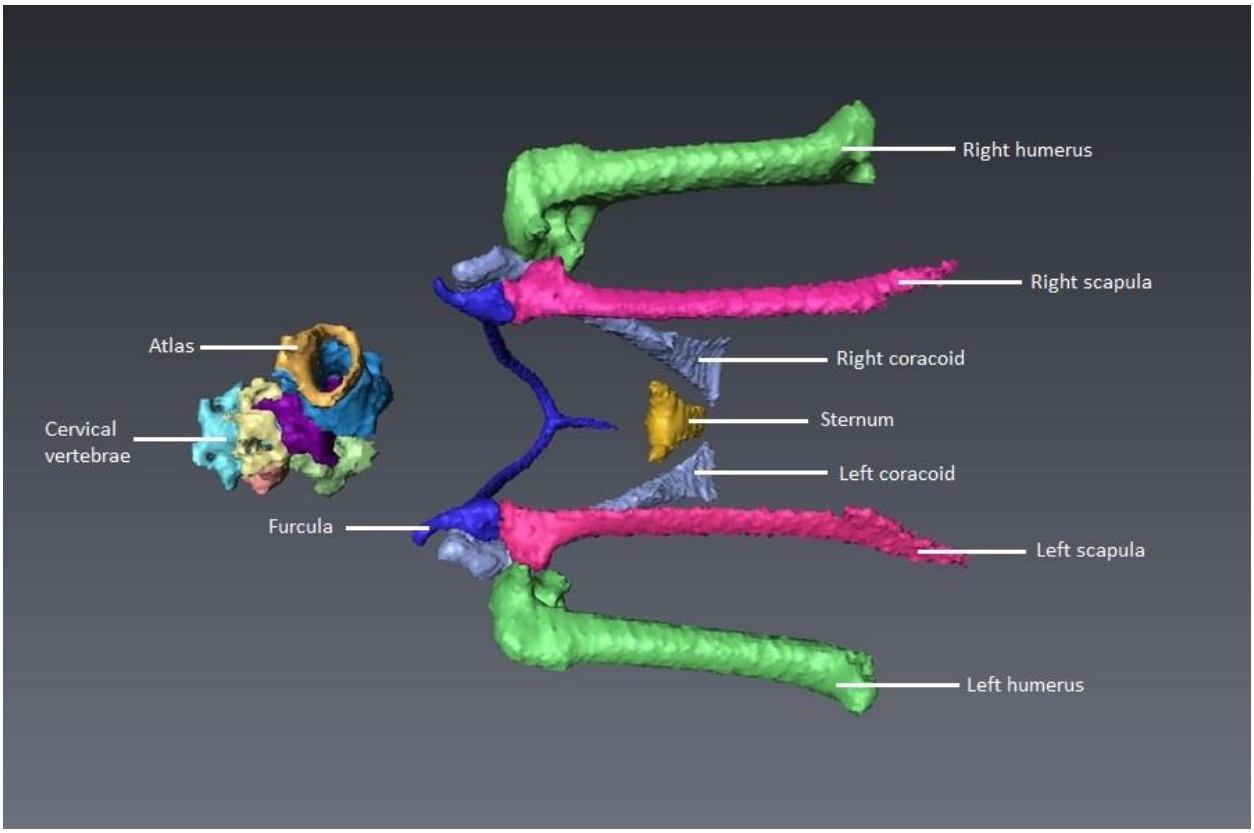

Figure 8: Screen shot of a surface generation rendering in Avizo® of a dorsal view of the segmented skeletal elements of the neck, shoulders, and upper forelimbs from an x-ray CT scan of a Bengalese Finch, *Lonchura striata* (DGH catalog #248).

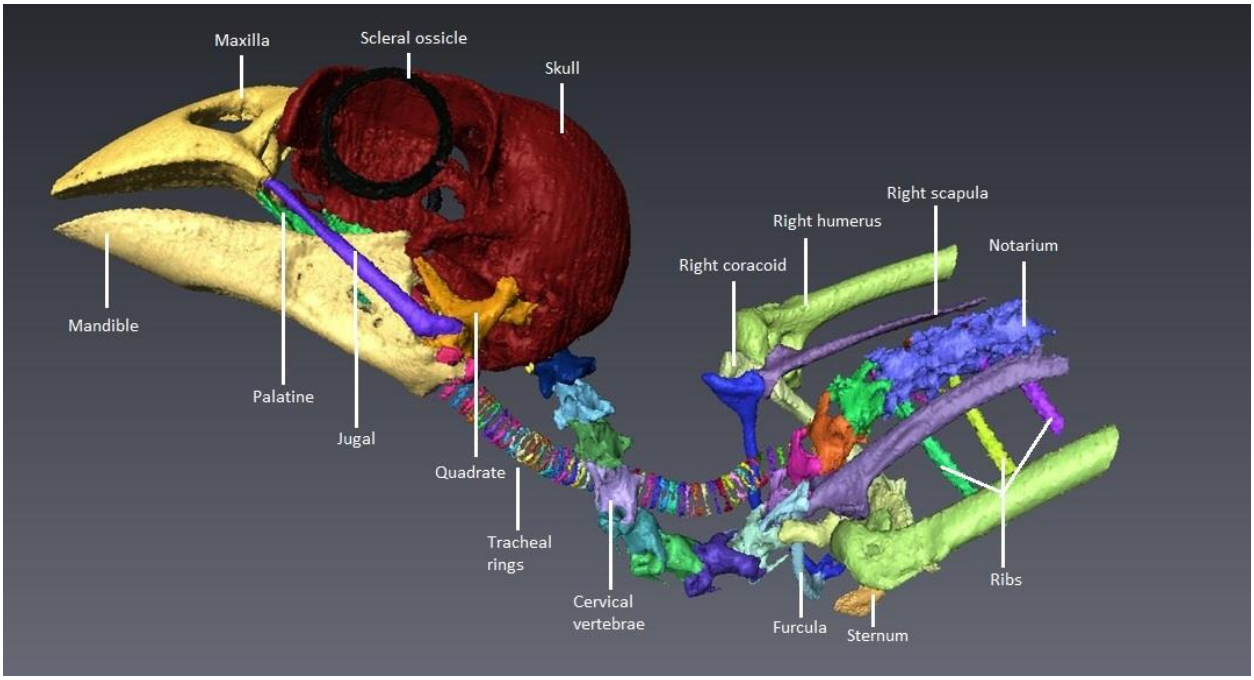

Figure 9: Screen shot of a surface generation rending in Avizo® of a lateral view of the skeletal elements of the head, trachea and upper neck and a dorso-lateral view of the skeletal elements of the shoulder region from an x-ray CT scan of a Northern Cardinal, *Cardinalis cardinalis* (DGH catalog #246).

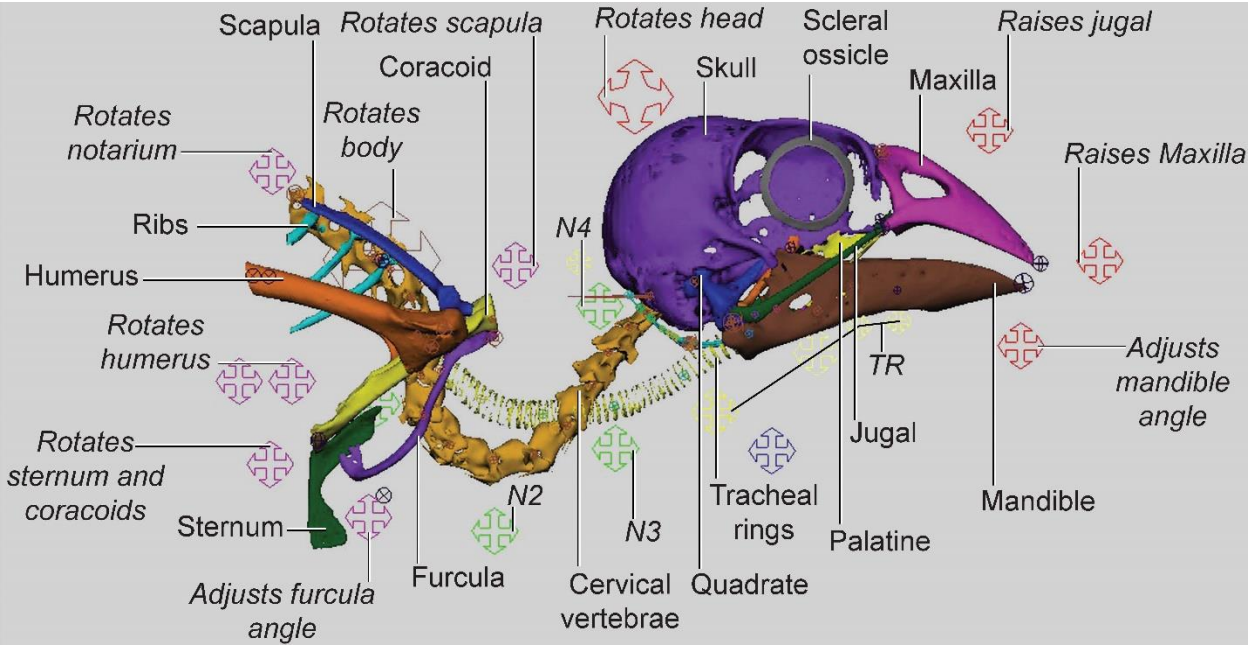

Figure 10: Screen shot of the 3D model of a Northern Cardinal, *Cardinalis cardinalis* (DGH catalog #246) imported into Maya®. The four-sided arrows represent movement controls in Maya®. The 4-sided arrows represent movement controls. N1-N4 control the rotation and bending of the vertebral column. TR controls the position of the tracheal rings and hyoid.

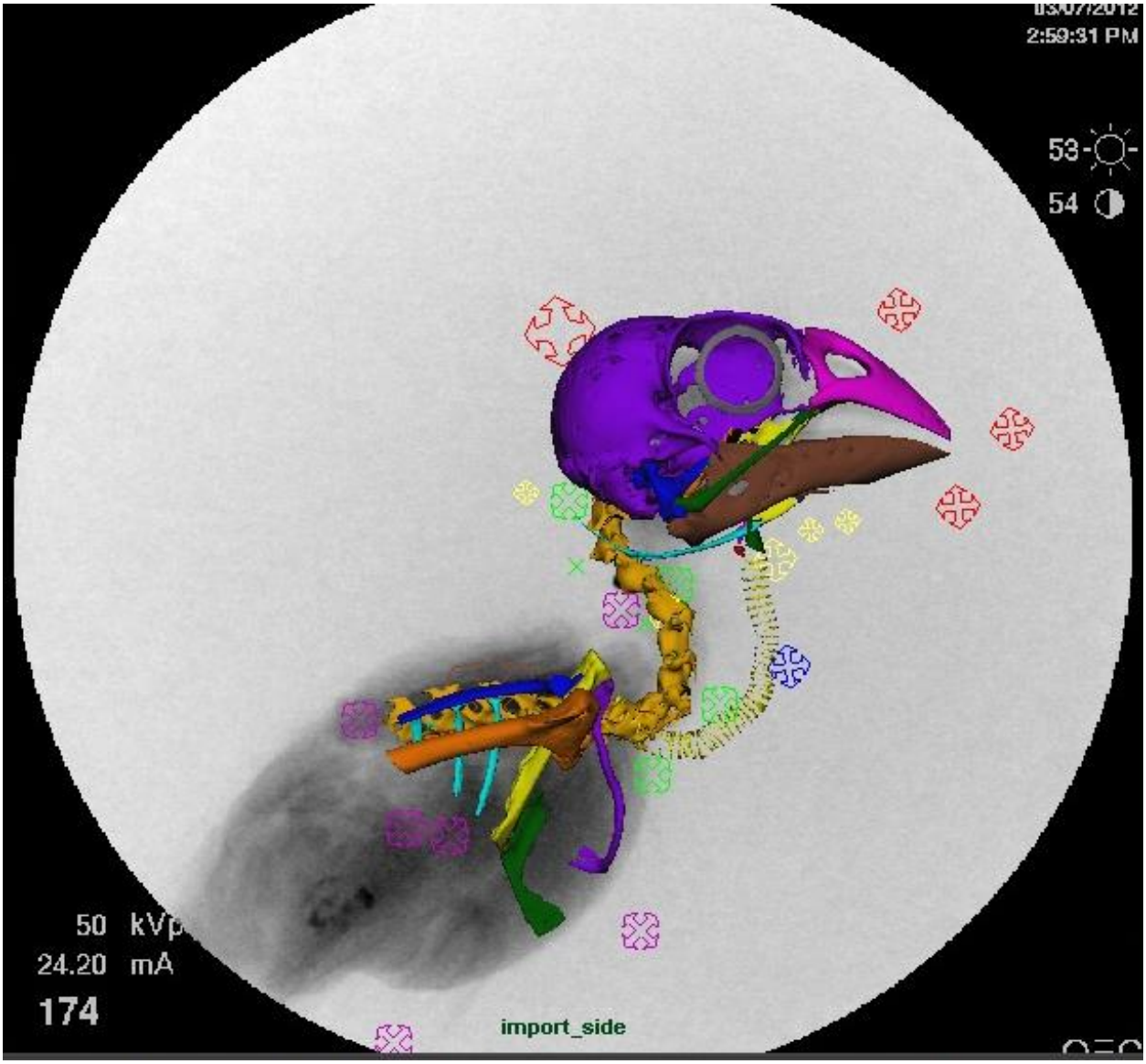

Figure 11: Screen shot of the 3D model of a Northern Cardinal, *Cardinalis cardinalis* (DGH catalog # 246) imported into Maya® and superimposed on a frame of an x-ray video (file name Car_542_13C; frame 10) of a Northern Cardinal, *Cardinalis cardinalis* (DGH catalog # 269). The skeletal elements of the 3D model have been moved to align with those in the x-ray background image.

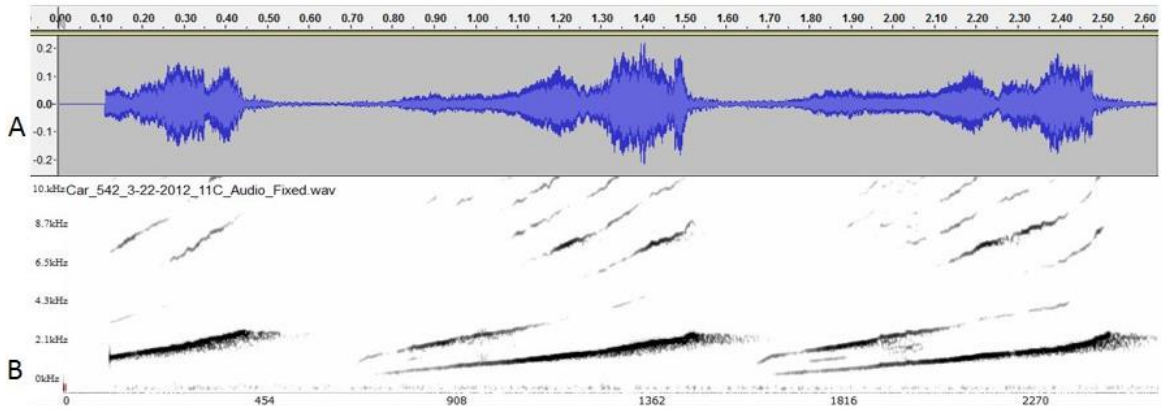

Figure 12: The amplitude waveform (A) and sonogram (B) created from the audio recording of a song of the Northern Cardinal, *Cardinalis cardinalis* (DGH catalog #246) (Roderick Suthers, unpublished data; used with permission).

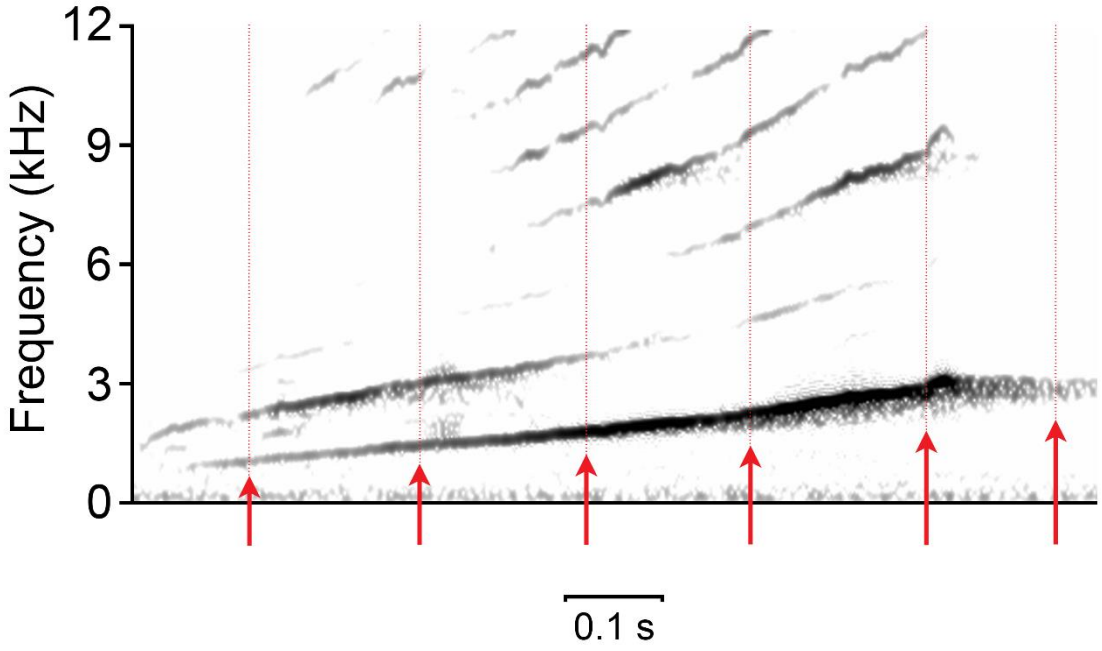

Figure 13: The second syllable of the sonogram created from the audio recording of a song of the Northern Cardinal, *Cardinalis cardinalis* (DGH catalog #246), which is synchronized with the x-ray video (Car_542_11C). The red arrows indicate the location of frames 39, 44, 49, 54, 59, and 63. (Roderick Suthers, unpublished data; used with permission).

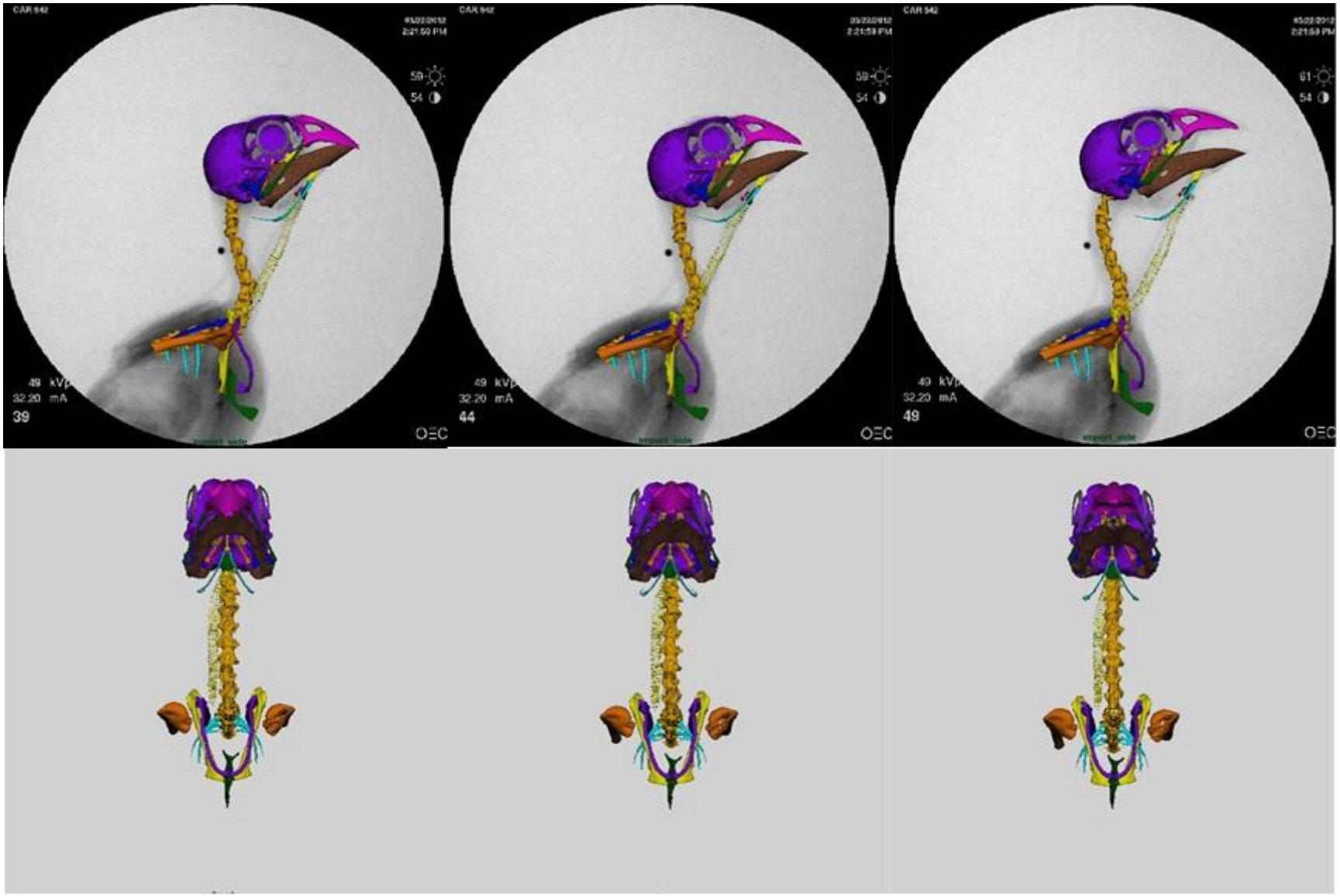

Figure 14A: Screen shot of the 3D model of a Northern Cardinal, *Cardinalis cardinalis* (DGH catalog # 246) imported into Maya® and superimposed on frames 39, 44, and 49 of an x-ray video (file name Car_542_11C; frame 10) of a Northern Cardinal, *Cardinalis cardinalis* (DGH catalog # 269).

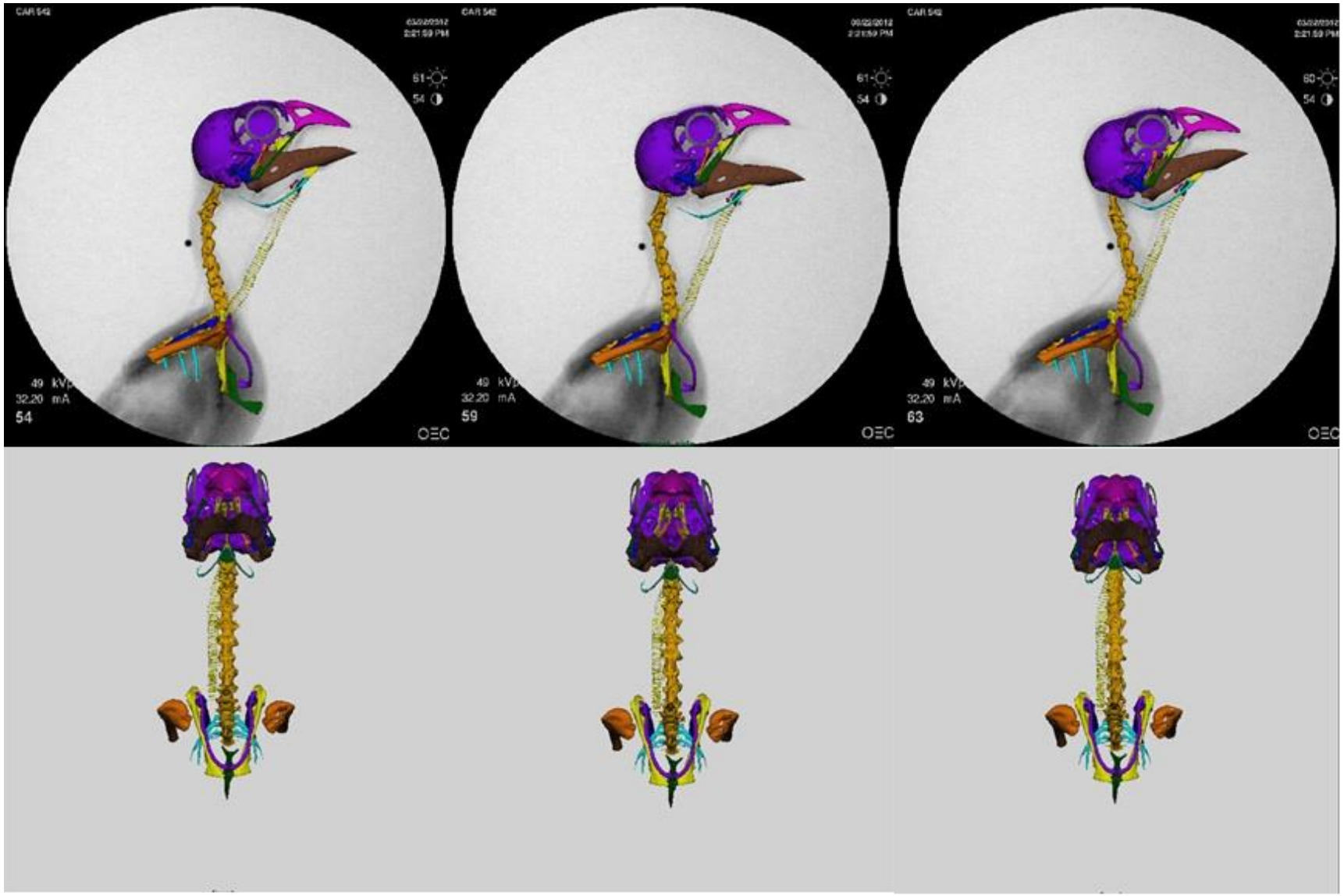

Figure 14B: Screen shot of the 3D model of a Northern Cardinal, *Cardinalis cardinalis* (DGH catalog # 246) imported into Maya® and superimposed on frames 54, 59, and 63 of an x-ray video (file name Car_542_11C; frame 10) of a Northern Cardinal, *Cardinalis cardinalis* (DGH catalog # 269).